Capacity and Coverage Analysis for FD-MIMO based THz Band 5G Indoor Internet of Things

Nabil Khalid, Naveed A. Abbasi and Ozgur B. Akan
Next-generation and Wireless Communications Laboratory
Department of Electrical and Electronics Engineering
Koc University, Istanbul, Turkey
Email: {nkhalid15, nabbasi13, akan}@ku.edu.tr

***Abstract*—Current and proposed Internet of things (IoT) applications are expected to bring about a major technological revolutions. Next-generation wireless communications in such devices are expected to support high speed data transfers. Among different candidate technologies, terahertz (THz) band communication seems to be a promising direction due to availability of high bandwidth in the electromagnetic spectrum around this frequency range and its directional nature governed by the directive antennas. In this paper, we look into some networking scenarios of full-dimension multiple-input multiple-output (FD-MIMO) based THz Band indoor wireless networks to determine the number of nodes that can be connected to a base station as a function of the antenna characteristics. Furthermore, we analyze the performance of the users and network based on their ergodic capacity. Our results suggest fundamental parameters that can be used in future THz Band analysis and implementations.**

***Index Terms*—5G indoor wireless networks, Terahertz (THz) channels, Capacity and coverage analysis, FD-MIMO, massive MIMO, Network density.**

I. Introduction

The inter-networking of devices, buildings, vehicles and other items such as wearable electronics that comprise technologies labeled under the banner of Internet of things (IoT), are quickly molding the future of technology in the current era. Cisco envisions this global phenomenon to reach a market value of more than 14 Trillion US Dollar by the year 2022 [1]. On the other hand, increasing data rates for communication are in high demand to cater for soaring data consumption in new applications such as high-resolution videos and 3D experience environments.

In order for the technology to compete with consumer needs, 5G wireless networks need to realize data rates reaching terabits per second (Tbps) [2], [3]. The 60 GHz spectrum is expected to increase data rates up to 6 Gbits/s [4] but the available spectrum around this frequency is limited to 2 GHz that may not completely satisfy the increasing demands of higher data rates. To support such high throughputs of Tbps, enormous bandwidth is required, and hence, researchers around the world are exploring the Terahertz (THz) Band (0.3 - 10 THz). Higher frequency networks can support higher data rates, however, being highly directional, they are more easily blocked by any obstacles on their path providing a set of unique challenges for THz Band communications. Additionally, IoT framework necessitate extensive and seamless communication between a large number of devices in indoor environment. Therefore, the main motivation for the current study is to provide analytical analysis for networking in THz Band communication systems such that they may be realized as an enabling technology for 5G indoor IoT applications.

978-1-5386-3531-5/17/$31.00

An efficient approach to increase system capacity using THz Band is to pack these directional antennas intelligently to form FD-MIMO such that the resulting array provides dedicated coverage to all the devices in its vicinity [5]. Several articles are available that analyze the performance of mmwave networks using directional antennas [6]. However, very limited literature is available that analyze the performance of FD-MIMO based THz Band network.

In this paper, our aim is to improve spatial multiplexing performance of THz Band networks by introducing a novel concept of spatial separation of antenna beams that is in addition to its half-power beam width (HPBW). We denote this separation parameter as guard width. To appreciate this concept in an FD-MIMO based THz Band network, we try to determine its effect on the user and network performance. We provide optimum guard width value for the scenario where user capacity is to be maximized and in the scenario where the network capacity is to be maximized. Expressions are derived for robust selection of guard width values and interpretation of the system performance. We also analyze the minimum cell separation required based on lowest possible inter-cell interference. An insight to the area spectral efficiency (ASE) of THz Band network is also provided to appreciate its use in the future indoor IoT applications.

The remainder of this paper is organized as follows. In Section II, we describe the system model used for simulation and performance analysis of THz Band network. Coverage and capacity modeling is provided in Section

III. Section IV discusses the analytical results. Finally, we conclude the paper in Section V.

II. System Model

Consider an indoor IoT network where devices achieve high speed bi-directional communication links by utilizing the capabilities of a THz Band channel and the base stations are equipped with FD-MIMO technology. Due to high path loss, the coverage area of THz Band networks is small, however, this peculiar behavior comes with an inherent advantage of smaller cell sizes that permit frequent channel reuse and more secure connections. To analyze such a network, we consider a scenario where the IoT devices are placed on the Eucledian plane, $\mathbb{R}^2$ with an average distance of r meters from the base station, as

$$r = \sum_{i=1}^{N} \frac{r_i}{N}, \tag{1}$$

where, r_i is the distance of i^{th} device and N is total number of devices connected to the base station.

A. FD-MIMO

A typical FD-MIMO system consists of an antenna array in 2-dimensional space that provides flexibility of beam-forming in almost any arbitrary direction. At lower frequency bands, the sizes of such antenna arrays become huge making their use in indoor IoT devices impractical. As an example, consider an antenna of 64 elements operating at 2.5 GHz in an 8×8 array with 0.5 wavelength (λ) separation. This would require a nominal area of 50 cm $\times$ 50 cm for the antenna array [5], which clearly is an infeasible solution for indoor IoT networks. On the other hand, at higher frequency, such as a THz Band system operating at 300 GHz, a similar array would require only 0.4 cm $\times$ 0.4 cm area. This is 20 times smaller than its lower frequency counterpart. Thus, THz Band is especially suited to FD-MIMO in indoor IoT networks.

By moving its beam, a typical planar antenna array can provide a coverage of 120° and multiple arrays can be placed in different orientations to increase the coverage [7]. Usually three arrays are placed in a triangular geometry to provide full 360° of coverage in a cell, as shown in Fig. 1. We denote the angular coverage of an antenna as antenna movement freedom (φ) and use it further in our analysis.

B. Antenna radiation pattern

Antenna radiation patterns play a very important role in determining the coverage of a system. In our analysis, antenna radiation pattern is approximated with a modified $sinc$ function. Such an antenna is characterized by the following three parameters; Half power beam width β_{3dB}, main lobe gain G_t and damping factor

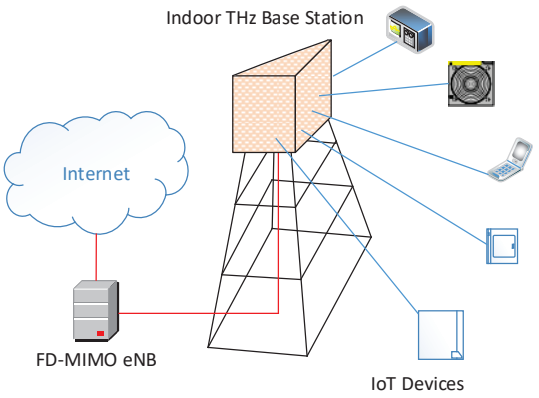

Fig. 1: THz Band FD-MIMO system.

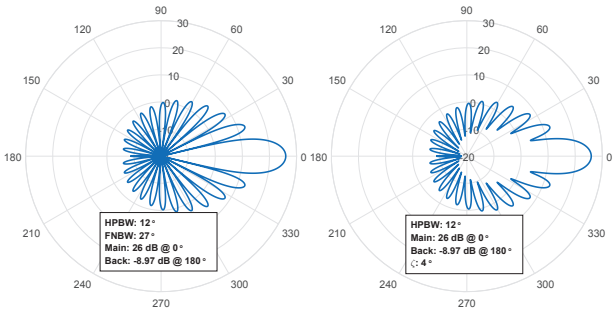

(a) (b)

Fig. 2: (a) Radiation pattern of the antenna based on ideal $sinc$ function (b) typical radiation pattern of the antenna with modified $sinc$ function.

ζ. The damping factor controls the sharpness of nulls and improve the realization of a $sinc$ function with an actual high directional antenna radiation pattern. Its value determines the number of neighboring points up to ζ degrees on either side of the specified $f(\theta)$.

The radiation pattern is modeled by the following expression,

$$f(\theta) = \frac{1}{2\zeta + 1} \sum_{m=-\zeta}^{\zeta} sinc^2(A\theta + m), \tag{2}$$

where, the value of A determines the lobe width dependent on β_{3dB} and can be determined considering θ_{3dB}, an angle where the function goes to the half value of its maximum,

$$sinc^2(A\theta_{3dB}) = 0.5, \tag{3}$$

$$\beta_{3dB} = 2\theta_{3dB} = \frac{0.8854}{A}, \tag{4}$$

hence,

$$A = \frac{0.8854}{\beta_{3dB}}. \tag{5}$$

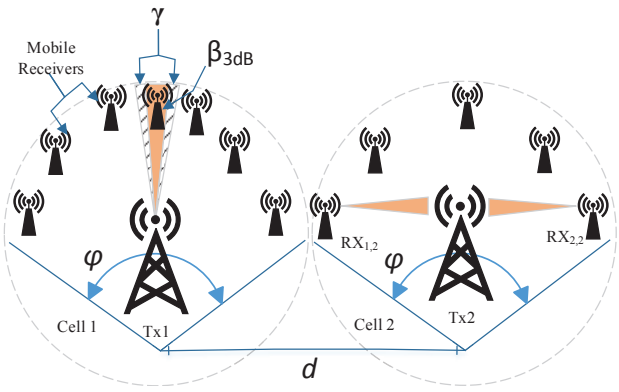

Fig. 3: THz Band FD-MIMO architecture.

The gain of the antenna at an arbitrary angle θ can be determined using,

$$G(\theta) = \frac{1}{2\zeta + 1} \sum_{m=-\zeta}^{\zeta} G_t \; sinc^2 \left(\frac{0.8854}{\beta_{3dB}} \, \theta + m \right). \tag{6}$$

The antenna radiation pattern using ideal $sinc$ function is shown in Fig. 2 (a). It can be seen from the figure that the pattern returns to null which does not represent a practical radiation pattern. A typical antenna radiation pattern is similar to the one shown in Fig. 2 (b) [8], which is used in our further analytical analysis.

As discussed earlier, thanks to the small antenna size at high frequency, many antennas can be packed to realize FD-MIMO and thus, multiple lobes can be spread around spatially to create several simultaneous communication links. However, very low inter-lobe spacing of antennas can cause severe interference among neighboring devices and downgrade the performance of spatial multiplexing. Using techniques derived from the principles of diffraction limited optics, similar to [9], one can significantly reduce the inter-lobe spacing, however, at the increased cost of system complexity. To avoid complexity, in this paper we propose a simpler system based on using the minimum gap between each lobe denoted as guard width (γ). We define γ as the angular distance between the β_{3dB} of adjacent lobes as shown in Fig. 3 and its optimal value is based on user requirements.

For a given φ, β_{3dB} and γ, number of possible connections (N) can be calculated using,

$$N = \left\lfloor \frac{\varphi}{\beta_{3dB} + \gamma} \right\rfloor, \tag{7}$$

where, $\lfloor \cdot \rfloor$ represents floor value of the expression.

C. Interference and Obstacles

Due to high directivity, THz Band networks are only LOS interference limited, which is why we include a guard width concept to enhance the node and network capacities.

Consider a scenario where the K^{th} user/receiver (K_r) is connected to the K^{th} transmitting beam (K_t). We assume that the receiver and transmitter beam are perfectly aligned to achieve maximum gain. This can be achieved by applying beam alignment technique on beam steering, which is essential to an FD-MIMO antenna array. Interference faced by the user K_r is due to the power transmitted by other lobes in the direction of this receiver. If neighboring beams are very close to a receiver, higher interference is faced by that node. Conversely, if the angular distance between each lobe is increased, it can be observed by looking at Fig. 2 (b) that the interference level will decrease, owing to the fact that transmission level gets weaker moving away from the main lobe at the expense of fewer devices per coverage area. The interference observed by a single user K_r can be determined as,

$$I_{K_r} = \sum_{i=1, i \neq K}^{N} G_{K_r} G_i(\theta_i) P_{t_i} \left(\frac{c}{4\pi f r} \right)^n, \tag{8}$$

where, $G_i(\theta_i)$ is the gain of transmitter i at an angle θ_i found using (6), G_{K_r} is the gain of user K_r, c is the speed of light, f is the frequency of transmission, r is the distance between the transmitter and the receiver and n is the path loss exponent. It should be noted here that the receiving antenna and the transmitting antenna array are assumed to be points on the Eucledian plane, $\mathbb{R}^2$ and the distance r is considered equal for all the transmitters. Also, G_{K_r} is considered to have maximum gain, irrespective of the angle θ_i.

It is evident from (7) that by decreasing γ, the number of connected user are increased, however, by (8) we can also see that this results in increased interference. The combination of both these behaviors directly influence the single-user and network-level capacities.

Due to high material absorption in the THz Band, obstructions have significant impact on the network performance. It is experimentally shown that the obstructions expected in THz Band can absorb transmitted signals in the range of 10-30 dB [10]. Considering that the obstruction between i^{th} transmitter and K^{th} receiver is denoted as $E(i, K)$, the resulting interference with obstruction can be written as,

$$I_{K_r} = \sum_{i=1, i \neq K}^{N} G_{K_r} G_i(\theta_i) P_{t_i} E(i, K) \left(\frac{c}{4\pi f r} \right)^n. \tag{9}$$

In this work, we consider the placement of obstructions as deterministic and leave the stochastic geometry analysis for future work.

III. Coverage and Capacity Model

In our system model, we consider that the base station is placed at the origin and that a node K_r receives signal

power which is determined by a simple variant of Friss path loss equation, as,

$$S_{K_r} = G_{K_r} G_{K_t} P_{t_K} E(i,K) \left(\frac{c}{4\pi f r}\right)^n, \qquad (10)$$

where, G_{K_t} and P_{t_K} is the gain and transmitted power of the K^{th} transmitter communicating with the K^{th} receiver, respectively. The user K has coverage if its Signal-to-interference-plus-noise-ratio (SINR) is greater than a threshold (T) that is required for successful packet transmission. The SINR for the stated system can be calculated as,

$$SINR = \frac{G_{K_r} G_{K_t} P_{t_K} E(i,K) \left(\frac{c}{4\pi f r}\right)^n}{N_0 + \sum\limits_{i=1, i\neq K}^{N} G_{K_r} G_i(\theta_i) P_{t_i} \left(\frac{c}{4\pi f r}\right)^n}. \qquad (11)$$

The threshold T is usually dependent on the modulation scheme being used in a system. The ergodic capacity of the system is given as [11],

$$C_{K_r} = B_c \, \log_2 (1 + SINR), \qquad (12)$$

where, B_c is the coherence bandwidth of the system. The parameter B_c is very important for wideband systems as it determines the range of frequencies for which the channel can be considered flat. It is affected by the multipath propagating signals that are usually expected in indoor channels.

Another important parameter, network capacity, in $\mathbb{R}^2$ can be calculated as,

$$NC_{\mathbb{R}^2} = N \cdot C_{K_r}, \qquad (13)$$

which determines the performance of the whole network. Moreover, the full FD-MIMO in $\mathbb{R}^3$ can be determined for the antennas with identical radiation pattern in azimuth and elevation directions as,

$$NC_{\mathbb{R}^3} = N_\theta N_\phi \cdot C_{K_r}, \qquad (14)$$

where, N_θ is evaluated by considering the $0 \leq \varphi_\theta \leq 360$ and β_{3dB_θ} for the azimuth plane of antenna array, while N_ϕ is evaluated by considering the $0 \leq \varphi_\phi \leq 180$ and β_{3dB_ϕ} for the elevation plane of the antenna array.

In this work, we have considered that each user is equally demanding the same capacity and thus, the parameter γ is identical for all users. For the case where each user demands different quality of service (QoS), this problem can be easily modified to assign a different γ value to each user and optimize it based on the maximum network capacity. We leave QoS based network optimization problem to the future work.

Next, we analyze the inter-cell distance (d) required in THz Band indoor wireless network. This important parameter is calculated based on the criterion of minimum inter-cell interference for a particular quality of communication. We determine this distance by considering the interference power received by two receiver orientations that are expected to be affected most by inter-cell interference. The first is a receiver placed closest to the cell boundary with its beam pointing in the opposite direction i.e. $G(180^\circ)$, $\text{RX}_{1,2}$ depicted in Fig. 3. While, the second is when a receiver being at the opposite end of the neighboring cell has its main beam pointing towards the local cell, $\text{RX}_{2,2}$ depicted in Fig. 3. Finally, minimum inter-cell distance is determined by making sure that the interference power is lower than the system noise floor for both the antenna orientations.

THz Band communications, due to its wide bandwidth, not only provides very high speed wireless communication, it also provides higher ASE due to smaller cell sizes such as femtocells. We determine the ASE by dividing the cell capacity with the network area.

$$ASE = \frac{NC_{\mathbb{R}^2}}{B_c \pi d^2}, \qquad (15)$$

where, d is the inter-cell distance between the two neighboring cells. This parameter determines how efficiently the frequency spectrum is used in THz Band indoor IoT network.

IV. Simulation Results

We first determine the interference signal level received by the user under examination as a function of guard width (γ) for multiple distances. This analysis gives us a first insight into the performance of the network. Simulations were performed using the parameters given in Table I. System bandwidth B_c was kept as 4.48 GHz which was determined experimentally in [12], [13] and the center frequency is set to 300 GHz. Thermal noise power of a 4.48 GHz band system at room temperature is -77.3 dBm and with a noise figure of 7 dB, the total noise power is -70.3 dBm. The value, -70 dBm in Table I is an approximate value. Gain of antenna used is 26 dBi with a HPBW of 12°, which is easily achievable in THz Band [10], [14], [15]. The path loss of 2 is statistically determined in previous experiments in [12]. Due to hardware limitations, generating high signal power is very difficult, however, 0 dBm of transmitter power is achievable as shown in [**?**] and hence used in our simulations. Antenna radiation pattern used in simulations was calculated using $\zeta = 4^\circ$. Finally, to satisfy the condition $K_r \leq N$, the receiver is always assigned a fixed value of $K_r = 1$.

The received interference signal power as a function of γ for different distances is calculated using (9) and shown in Fig. 4 (a). As expected, it can be seen that the interference signal power decreases with increasing γ. However, an interesting point to be noted here is that there are also some smaller values of γ where the interference drops significantly. This enhancement is due to the suitable placement of the nulls of neighboring

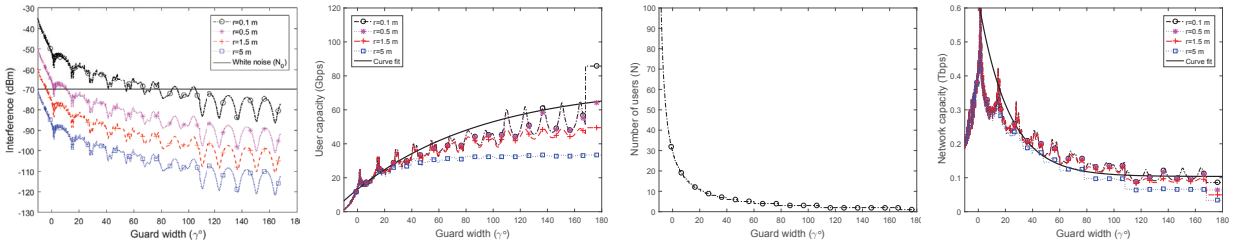

(a) (b) (c) (d)

Fig. 4: Simulation results for (a) total interference power received by the UE for different γ values, (b) capacity of single user for different γ values and distances, (c) maximum number of users at a given γ and (d) capacity of the network for different γ values and distances.

TABLE I: Setup parameters.

Parameter	Symbol	Value
Bandwidth	B_c	4.48 GHz
Frequency	f	300 GHz
Speed of light	c	299792458 m/s
Average distance	r	0.1, 0.5, 1.5, 5 m
White noise	N_0	-70 dBm
Gain	G	26 dBi
HPBW	β_{3dB}	12°
Path loss exponent	n	2
Transmitter power	P_t	0 dBm
Pattern smoothing	ζ	4°
Receiver	K_r	1

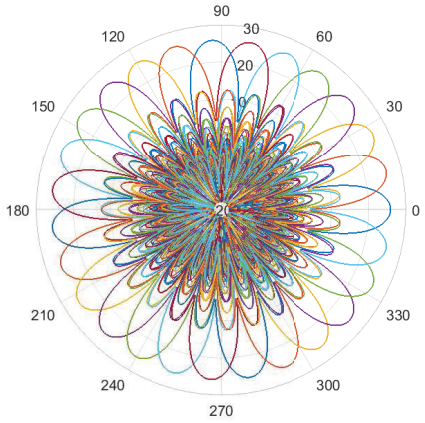

Fig. 5: Radiation pattern FD-MIMO with $\gamma = 1.32°$.

beams. It can be inferred that these point can produce interesting results by providing low interference even at smaller γ. Furthermore, at smaller distance the interference signal power is higher than the white noise N_0 for lower γ values, while, for distances greater than 1.5 m, the interference signal power gets lower than the N_0 and hence, will not effect the performance of the receiver. It should be noted here that the negative values of γ depicts the separation between the beams to be even less than the β_{3dB}.

We further examine the effect of γ by determining user capacity in our system by using (12) for different distances. It can be seen in Fig. 4 (b) that by using the proposed system, we can achieve very high data transmission speed. The user capacity reaches its maximum at 168.1°. Whereas the spikes in the results confirm that the proper placement of the nulls of neighboring beams can be very advantageous for the system as it provides higher SINR at lower γ. Further, we have evaluated an exponential approximation curve that represents the user capacity by $(-61.24e^{-0.01049\gamma} + 74.43) \times 10^9$. This curve fit is used to analyze the system performance trade-off when combined with other curves that are discussed later.

Although the results show that user capacity is increased by increasing γ, (7) suggests that the number of possible user connections will decrease. This attribute is also shown in Fig. 4 (c) and it also depicts that the value of γ directly influence the full network performance and therefore, must be carefully determined.

Next we determine the network performance by using (13). It can be seen in Fig. 4 (d) that the network performance degrades exponentially as γ increases which is due to the fact that the number of possible user connections are decreased. It should be noted here that, for negative values of γ, the network capacity reduces significantly. This is due to the fact that the interference at negative values of γ is very high and thus, a higher number of users does not increase the over all network performance. The optimum network capacity is achieved at $\gamma = 1.32°$. Here, we again provide a curve fit that approximates the network capacity using an exponential equation $(0.5205e^{-0.045\gamma} + 0.1037) \times 10^{12}$. Finally, as in the earlier cases, we again see spikes in the results occurring due to the suitable placement of the nulls in the network capacity. To further investigate this behavior, we present the radiation pattern of the transmitter at $\gamma = 1.32°$ in Fig. 5. Although, in practice, such precise placement of antenna might seem difficult, it is possible to place the antenna beams on precise locations by using advanced beam steering techniques as shown in [17].

It is now evident that a suitable selection of γ is very

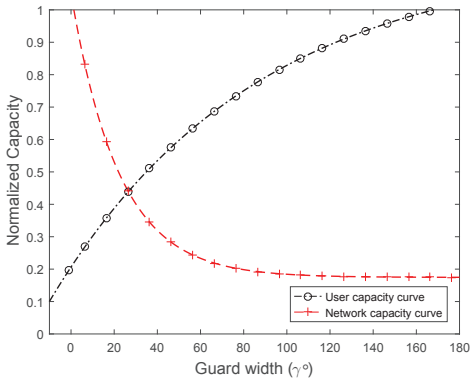

Fig. 6: Normalized capacity curves to find optimum Guard width (γ) based on the requirements.

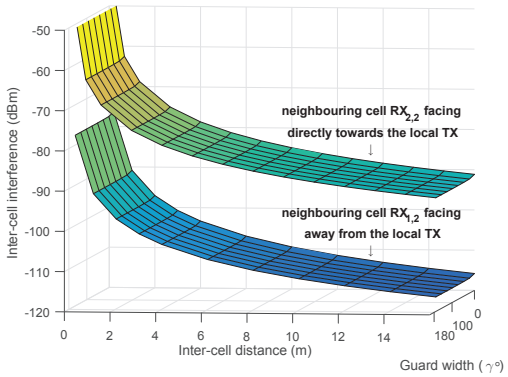

Fig. 7: Distance required for minimum inter-cell interference.

important for FD-MIMO systems. Hence, to visualize the trade-off process for selecting optimal γ in any scenario, we provide the normalized curve fit graphs of user capacity and network capacity in Fig. 6. For instance, in case a guard width of 1.32° is selected, the network performance is optimum, however, the graph depicts that the user performance will be 22% of the maximum performance. An interesting value is where both the curves intersect each other at $\gamma = 27^\circ$. This point is the balanced optimum for both the parameters, as both are operating at 44.26% of their respective maximum values. Similarly, in cases where the objective is to optimize user capacity, $\gamma = 168.1^\circ$ must be used, while the network performance at this γ will be 17.5%. These curves can significantly help in developing optimization algorithms required for FD-MIMO based THz Band indoor IoT networks.

Due to higher path loss, THz Band network provides higher frequency reuse. To determine the minimum inter-cell distance, we observe the interference signal power received by two receivers of the neighboring cell. The results for both the receivers are shown in Fig. 7. It can be seen that the neighboring cell receiver facing in the opposite direction receives an interference signal that stays mostly below the system white noise N_0. Hence to determine the inter-cell distance, we ensure that the power of interference signal received by the neighboring cell receiver facing directly toward the local receiver remains below -70 dBm. We can observe from Fig. 7 that at an inter-cell distance of 1.6 m, the interference power goes below the white noise N_0.

Finally, we determine the ASE of FD-MIMO based THz Band network. For an inter-cell distance of 1.6 m and $\gamma = 1.32^\circ$, the ASE reaches up to 4.6 b/s/Hz/m^2 as shown in Fig. 8. The ASE of THz Band network is much higher compared to lower frequency networks and can significantly help alleviating high data rates problem in future indoor 5G networks [10].

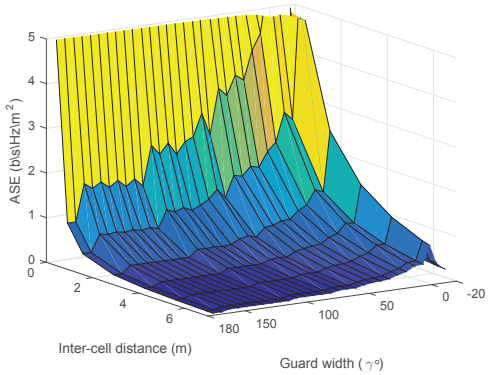

Fig. 8: Change in area spectral efficiency based on inter-cell distance.

V. Conclusion

In this paper, we presented an analysis based on a novel node separation scheme to characterize the performance of future THz Band IoT networks. We presented the concept of guard width (γ), that is a beam separation in access to the antenna HPBW, to mitigate the effect of interference. By applying this concept on a THz Band network, we analyzed interference as well as user and network performance to determine the optimum value of guard width in a number of scenarios. We also presented a trade-off that may assist in robust selection of guard width based on the target IoT applications. We have shown that nodes operating in THz Band can reach tens of Gbps speed while the networks can provide Tbps which is an order-of-magnitude more speed as compared to lower frequency networks. In addition to the stated parameters, we have also determined the minimum inter-cell distance required in a THz Band network and shown that it can accommodate a high number of users. Finally, we have shown the area spectral efficiency of the network can reach 1000 times more than the lower frequency networks by using optimum guard

width values.

VI. Acknowledgment

This work was supported in part by the Scientific and Technological Research Council of Turkey (TUBITAK) under grant $\#113E962$.

References

[1] J. Bradley, J. Barbier, and D. Handler, "Embracing the internet of everything to capture your share of $14.4 trillion," *White Paper, Cisco*, 2013.

[2] K.-C. Huang and Z. Wang, "Terahertz terabit wireless communication," *Microwave Magazine, IEEE*, vol. 12, no. 4, pp. 108–116, June 2011.

[3] R. Daniels and R. Heath, "60 ghz wireless communications: emerging requirements and design recommendations," *Vehicular Technology Magazine, IEEE*, vol. 2, no. 3, pp. 41–50, Sept 2007.

[4] IEEE, "Part 15.3: Wireless medium access control and physical layer specifications for high rate wireless personal area networks," *IEEE*, 2009.

[5] Y. Kim, H. Ji, J. Lee, Y. H. Nam, B. L. Ng, I. Tzanidis, Y. Li, and J. Zhang, "Full dimension mimo (fd-mimo): the next evolution of mimo in lte systems," *IEEE Wireless Communications*, vol. 21, no. 2, pp. 26–33, April 2014.

[6] A. Thornburg, T. Bai, and R. W. Heath, "Mmwave ad hoc network coverage and capacity," in *2015 IEEE International Conference on Communications (ICC)*, June 2015, pp. 1310–1315.

[7] Y. H. Nam, B. L. Ng, K. Sayana, Y. Li, J. Zhang, Y. Kim, and J. Lee, "Full-dimension mimo (fd-mimo) for next generation cellular technology," *IEEE Communications Magazine*, vol. 51, no. 6, pp. 172–179, June 2013.

[8] C. Balanis, *Antenna Theory: Analysis and Design*. Wiley, 2016. [Online]. Available: https://books.google.com.tr/books?id=iFEBCgAAQBAJ

[9] N. Khalid and O. B. Akan, "Experimental throughput analysis of low-thz mimo communication channel in 5g wireless networks," *IEEE Wireless Communications Letters*, vol. 5, no. 6, pp. 616–619, Dec 2016.

[10] ——, "Wideband thz communication channel measurements for 5g indoor wireless networks," in *2016 IEEE International Conference on Communications (ICC)*, May 2016, pp. 1–6.

[11] C. Shannon, "A mathematical theory of communication," *Bell System Technical Journal, The*, vol. 27, no. 3, pp. 379–423, July 1948.

[12] S. Kim and A. G. Zaji, "Statistical characterization of 300-ghz propagation on a desktop," *IEEE Transactions on Vehicular Technology*, vol. 64, no. 8, pp. 3330–3338, Aug 2015.

[13] S. Priebe, M. Kannicht, M. Jacob, and T. Krner, "Ultra broadband indoor channel measurements and calibrated ray tracing propagation modeling at thz frequencies," *Journal of Communications and Networks*, vol. 15, no. 6, pp. 547–558, Dec 2013.

[14] W. Roh, J. Y. Seol, J. Park, B. Lee, J. Lee, Y. Kim, J. Cho, K. Cheun, and F. Aryanfar, "Millimeter-wave beamforming as an enabling technology for 5g cellular communications: theoretical feasibility and prototype results," *IEEE Communications Magazine*, vol. 52, no. 2, pp. 106–113, February 2014.

[15] C. Lin and G. Y. Li, "Indoor terahertz communications: How many antenna arrays are needed?" *IEEE Transactions on Wireless Communications*, vol. 14, no. 6, pp. 3097–3107, June 2015.

[16] I. Kallfass, I. Dan, S. Rey, P. Harati, J. Antes, A. Tessmann, S. Wagner, M. Kuri, R. Weber, H. Massler, A. Luether, T. Merkle, and T. Kurner, "Towards mmic-based 300ghz indoor wireless communication systems," *IEICE Transactions on Electronics*, vol. E98.C, no. 12, pp. 1081–1090, 2015.

[17] B. Sadhu, Y. Tousi, J. Hallin, S. Sahl, S. Reynolds, . Renstrm, K. Sjgren, O. Haapalahti, N. Mazor, B. Bokinge, G. Weibull, H. Bengtsson, A. Carlinger, E. Westesson, J. E. Thillberg, L. Rexberg, M. Yeck, X. Gu, D. Friedman, and A. Valdes-Garcia, "7.2 a 28ghz 32-element phased-array transceiver ic with concurrent dual polarized beams and 1.4 degree beam-steering resolution for 5g communication," in *2017 IEEE International Solid-State Circuits Conference (ISSCC)*, Feb 2017, pp. 128–129.